[CANCER RESEARCH 63, 3403–3412, June 15, 2003]

Tumor-derived Vascular Endothelial Growth Factor Up-Regulates Angiopoietin-2 in Host Endothelium and Destabilizes Host Vasculature, Supporting Angiogenesis in Ovarian Cancer[1]

Lin Zhang, Nuo Yang, Jin-Wan Park, Dionyssios Katsaros, Stefano Fracchioli, Gaoyuan Cao, Ann O'Brien-Jenkins, Thomas C. Randall, Stephen C. Rubin, and George Coukos[2]

Abramson Family Cancer Research Institute [L. Z., G. Co.], Center for Research on Reproduction and Women's Health [L. Z., J-W. P., A. O-J., G. Co.], Division of Gynecologic Oncology, Department of Obstetrics and Gynecology [T. C. R., S. C. R., G. Co.], Cell and Molecular Biology Program and Department of Genetics [N. Y.], Division of Pulmonary, Allergy and Critical Care, Department of Medicine [G. Ca.], University of Pennsylvania, Philadelphia, Pennsylvania 19104, and Department of Obstetrics and Gynecology, University of Turin, Turin, Italy [D. K., S. F.]

ABSTRACT

Vascular remodeling in host tissues surrounding growing tumors is implicated in the successful development of tumor neovasculature. Cooperation between vascular endothelial growth factor (VEGF) and angiopoietins (Angs) is considered to be critical in this context. However, the mechanisms regulating the coordinated expression of these molecules remain, to date, elusive. In this study, we used a murine ovarian cancer angiogenesis model induced by overexpression of VEGF, as well as 52 human ovarian cancer specimens and 36 established cancer cell lines to characterize the expression and regulation of Ang-2 in the context of tumor angiogenesis. Using a combination of immunohistochemistry, laser capture microdissection and real-time quantitative reverse transcription-PCR, we showed that tumor-derived VEGF significantly up-regulated the expression of Ang-2 in host stroma endothelial cells, resulting in markedly increased Ang-2/Tie-2 mRNA copy number ratio *in vivo*. *In vitro* experiments showed that VEGF directly up-regulated Ang-2, which is mediated via VEGF receptor-2/flk-1/KDR pathway, in cultured endothelial cells through transcriptional activation rather than the enhanced mRNA stability. In human ovarian cancer, Ang-2 was primarily expressed in stroma endothelial cells and detectable in tumor cells of only 12% tumor specimens; however, it was not detected in the majority of established ovarian cancer cell lines. In addition, a significant correlation was observed between VEGF and Ang-2 mRNA expression ($P < 0.01$) but not between VEGF and Ang-1 or Tie-2 in human ovarian cancer specimens. In the mouse ovarian cancer model, up-regulation of Ang-2 in host stroma endothelial cells was significantly associated with pericyte loss and instability of the host vasculature surrounding the tumor. Our study suggests a novel mechanism by which tumor-derived VEGF interacts with Angs/Tie-2 system in host stroma endothelial cells and induces in a paracrine manner the remodeling of host vasculature to support angiogenesis during tumor growth.

INTRODUCTION

Tumor growth is angiogenesis dependent (1). Solid tumors cannot grow beyond 1–3 mm^3 without being subject to hypoxia. The subsequent activation of hypoxia-inducible factor up-regulates the expression of vascular endothelial growth factor (VEGF),[3] which switches on the angiogenic process by promoting endothelial cell proliferation and migration (2–6). VEGF is regarded as one of the earliest signals to stimulate the multistep cascade of tumor angiogenesis (6). Although various molecules are involved in this angiogenic switch, VEGF and the Ang family have been proposed to play a predominant role (6) because they are the only known growth factors largely specific for vascular endothelial cells.

Central to the successful development of tumor neovasculature is the remodeling of preexisting vasculature in host tissues surrounding the growing tumor mass. Such vessels enlarge and actively engage in sprouting and branching to meet the metabolic demands of adjacent malignancy (2–6). The molecular mechanisms underlying the remodeling of host vasculature remain, to date, elusive. Tumor cells play a paramount role in altering the balance of pro- and antiangiogenic molecules (3), and accumulating evidence indicates that the cooperation between VEGF and Angs may play a critical role in this context. Ang-1 maintains and stabilizes mature vessels by promoting the adhesive interactions between endothelial cells and surrounding cells, whereas Ang-2 might serve as a natural antagonist of constitutive Ang-1 signaling (2, 7). During development, VEGF promotes primitive vessel formation, and Ang-1 remodels and stabilizes these vessels (8). In adults, destabilization by Ang-2 in the absence of VEGF has been proposed to result in vessel regression, whereas such destabilization in the presence of high VEGF levels facilitates the angiogenic response (9, 10). In fact, Ang-2 can cooperate with VEGF to induce angiogenesis, whereas Ang-1 can offset VEGF-induced angiogenesis *in vivo* (11). During tumor angiogenesis, both distinct and overlapping expression patterns of VEGF and Angs have been reported, and vessel destabilization by Ang-2 in the presence of VEGF has been hypothesized to induce tumor angiogenesis (9, 12).

Such synergistic effect of VEGF and Angs in angiogenesis implies certain hitherto unknown mechanisms regulating temporally and spatially the coordinated expression of both molecules, affording their concurrent or sequential effect on tumor angiogenesis. Our current knowledge on the coordinated expression and regulation of VEGF and Angs is very limited. Ang-2 is expressed by endothelial cells of normal tissues or tumor (8, 12). The close correlation observed between VEGFR-2/flk-1/KDR and Ang-2 in tumor-associated endothelium (13) suggests that the VEGF/VEGFR-2 system may be involved in the regulation of Ang-2. Interestingly, both VEGF and hypoxia have been shown to up-regulate the expression of Ang-2 in cultured bovine endothelial cells (14, 15). Collectively, these reports indicate that tumor-derived VEGF might be implicated in the regulation of Ang-2 in endothelial cells in tumors and, consequently, in the remodeling of the host vasculature.

To investigate the role of tumor-derived VEGF in regulating the expression of Ang-2 and promoting instability in tumor-associated vessels *in vivo*, we used a syngeneic murine ovarian cancer model overexpressing VEGF164, which was recently generated in our

Received 12/19/02; accepted 4/16/03.

The costs of publication of this article were defrayed in part by the payment of page charges. This article must therefore be hereby marked *advertisement* in accordance with 18 U.S.C. Section 1734 solely to indicate this fact.

[1] Supported by grants by the American Association of Obstetricians and Gynecologists' Foundations, National Cancer Institute Ovarian Grant SPORE P01-CA83638, institutional funding from the Abramson Family Cancer Center and Cancer Research Institute, and the Department of Obstetrics and Gynecology at the University of Pennsylvania.

[2] To whom requests for reprints should be addressed, at Center for Research on Reproduction and Women's Health, 1355 Biomedical Research Building II/III, 421 Curie Boulevard, Philadelphia, PA 19104. Phone: (215) 746-7798; Fax: (215) 573-7627; E-mail: gcks@mail.med.upenn.edu.

[3] The abbreviations used are: VEGF, vascular endothelial growth factor; Ang, angiopoietin; VEGFR, VEGF receptor; FBS, fetal bovine serum; HUVEC, human umbilical vein endothelial cell; RT-PCR, reverse transcription-polymerase chain reaction; GAPDH, glyceraldehyde-3-phosphate dehydrogenase; IHC, immunohistochemistry; α-SMA, smooth muscle actin α; LCM, laser capture microdissection; CM, conditioned media.

laboratory (16). Here, we demonstrate that tumor-derived VEGF remarkably up-regulates Ang-2 expression in endothelial cells of the tumor stroma and adjacent host tissues in a paracrine manner and that this effect is mediated by VEGFR-2. Tumor-derived VEGF also results in a relative increase of Ang-2 to Ang-1, and this altered Ang balance in favor of Ang-2 in combination with the VEGF expression is associated *in vivo* with the loss of pericyte support, dramatically enhanced angiogenesis, and accelerated tumor growth.

MATERIALS AND METHODS

Cell Culture. A total of 36 human cancer cell lines and H5V, a murine-immortalized heart endothelial cell line (17), was cultured in DMEM supplemented with 10% FBS (Invitrogen, Carlsbad, CA). HUVECs (Clonetics, San Diego, CA) were cultured on gelatin as described elsewhere (18) and used between passages 2 and 6. ID8 cells (19) were maintained in DMEM supplemented with 4% FBS.

Retroviral Vector Construction and Infection. The retroviral vector containing murine VEGF164/GFP as well as the ID8 cell line stably overexpressing VEGF164/GFP or GFP were generated as described previously (16).

***In Vitro* Treatment of Endothelial Cells.** H5V cells and HUVECs were seeded in 6-well plates and cultured in the corresponding complete media. Upon reaching 90% confluence, H5V cells and HUVECs were cultured in 0.5 and 5% FBS-reduced media, respectively, for 8 h to decrease the effect of growth factors present in the complete media. In some experiments, H5V cells and HUVECs were incubated for 6 h in the presence of recombinant mouse VEGF164 (R&D Systems, Minneapolis, MN) or human VEGF165 (Peprotech, Rocky Hill, NJ), respectively, in serum-reduced culture media with or without SU1498 (15 μM; Calbiochem, San Diego, CA). In some experiments, H5V cells and HUVECs were incubated for 6 h in supernatants of ID8 cells transfected by VEGF164/GFP or control GFP virus. CM were collected every 24 h from 80% confluent cultures. All experiments were repeated at least three times.

Animals and *in Vivo* Tumor Generation. Six to 8-week-old female C57BL/6 mice were used in protocols approved by the Institutional Review Board of the Wistar Institute and the University of Pennsylvania. Transplantable syngeneic ID8 ovarian cancer s.c. model was generated as described previously (16).

Human Ovarian Cancer Specimens. Stage I ($n = 9$) and stage III or IV ($n = 43$) ovarian carcinoma specimens were randomly selected from the human tissue bank existing in our laboratory (20). The specimens used in this study have been collected at the University of Pennsylvania Medical Center from 2000 to present after obtaining appropriate written informed consent under Institutional Review Board-approved protocols or at the University of Turin, (Turin, Italy) between 1991 and 1999 after obtaining appropriate verbal informed consent under Institutional Review Board-approved protocols.

RNA Isolation and RT-PCR. Total RNA was isolated from 1×10^6 cultured cells or 100–500 mg of frozen tissue with TRIzol reagent (Invitrogen). After treatment with RNase-free DNase (Invitrogen), RNA was additionally purified with RNeasy RNA isolation kit (QIAgen, Valencia, CA). Total RNA was reverse transcribed using Superscript First-Strand Synthesis Kit for RT-PCR (Invitrogen) under conditions described by the supplier. Reverse-transcribed cDNA was amplified in 25 μl of PCR reaction system with Taq core PCR kit (Roche, Indianapolis, IN).

Quantitative Real-Time RT-PCR. cDNA was quantified by real-time PCR on the ABI Prism 7700 Sequence Detection System (Applied Biosystems, Foster City, CA). PCR was performed using Taqman PCR core reagents or Sybr Green PCR core reagent (Applied Biosystems) according to manufacturer's instructions. Specific oligonucleotide primers and probes (Table 1) were designed based on published sequences. To avoid false-positive results attributable to the amplification of contaminated genomic DNA in the cDNA preparation, all primers were designed to reside on exons separated by an intron. A novel set of primers and Taqman probe for quantification of all murine VEGF isoforms by real-time RT-PCR were used as described previously (21, 22). PCR amplification of the housekeeping gene, GAPDH, was performed for each sample as control for sample loading and to allow normalization among samples. A standard curve was constructed with PCR-II TOPO cloning vector (Invitrogen) containing the same inserted fragment and amplified by the real-time PCR. Each sample was run twice, and each PCR experiment included two nontemplate control wells. PCR products were confirmed as single bands using gel electrophoresis. The absolute copy number of some target genes were calculated as described previously (21).

Table 1 *Primer sequences*

Primer name	Sequence
mVEGF outer F	GAA GTC CCA TGA AGT GAT CAA G
mVEGF outer R	TCA CCG CCT TGG CTT GTC A
mVEGF common F	GCC AGC ACA TAG AGA GAA TGA GC
mVEGF120 R	CGG CTT GTC ACA TTT TTC TGG
mVEGF164 R	CAA GGC TCA CAG TGA TTT TCT GG
mVEGF188 R	AAC AAG GCT CAC AGT GAA CGC T
mVEGF common probe	ACA GCA GAT GTG AAT GCA GAC CAA AGA AAG
mGAPDH F	CCT GCA CCA CCA ACT GCT TA
mGAPDH R	TCA TGA GCC CTT CCA CAA
mGAPDH probe	CCT GGC CAA GGT CAT CCA C
mCD31 F	GTT CAC CTT CTG TGA GGA GAT GG
mCD31 R	ATC TCC AGC GCA CTC TTG CTA T
mflt-1 F	ACC TGT CCA ACT ACC TCA AGA GC
mflt-1 R	CTG GTT CCA GGC TCT CTT TCT T
mKDR/flk-1 F	CGA CAT AGC CTC CAC TGT TTA TG
mKDR/flk-1 R	TTT GTT CTT GTT CTC GGT GAT GT
mNeuropilin-1 F	ATT TGA AGT TTA TGG CTG CAA GA
mNeuropilin-1 R	ATT GGA TGC TGT AAT CTG GGA GT
mAng-1 F	CCA TGC TTG AGA TAG GAA CCA G
mAng-1 R	TTC AAG TCG GGA TGT TTG ATT T
mAng-2 F	AGC AGA TTT TGG ATC AGA CCA G
mAng-2 R	GCT CCT TCA TGG ACT GTA GCT G
mTie-1 F	TGG AGT CCA CTG TGA AAA GTC A
mTie-1 R	GCA TCG TCC CTA TGT TGA AC TC
mTie-2 F	CGG CTT AGT TCT CTG TGG AGT C
mTie-2 R	GGC ATC AGA CAC AAG AGG TAG G
hVEGF F	AAC CAT GAA CTT TCT GCT GTC TTG
hVEGF R	TTC ACC ACT TCG TGA TGA TTC TG
hAng-1 F	GTT AAT GGA CTG GGA AGG GAA C
hAng-1 R	GCT GTC CCA GTG TGA CCT TTT A
hAng-2 F	AGA TTT TGG ACC AGA CCA GTG A
hAng-2 R	GGA TGA TGT GCT TGT CTT CCA T
hTie-2 F	GTT CTG TCT CCC TGA CCC CTA T
hTie-2 R	TAA GCT TAC AAT CTG GCC CGT A
hGAPDH F	CCT GCA CCA CCA ACT GCT TA
hGAPDH R	CAT GAG TCC TTC CAC GAT ACC A
hGAPDH probe	CCT GGC CAA GGT CAT CCA C

mRNA Stability Assay. After incubation with VEGF or VEGF plus SU1498 for 2 h, the transcription inhibitor actinomycin D (Sigma, St. Louis, MO) was added to the culture media at a concentration of 7.5 μg/ml. Total mRNA was isolated at 0, 2, 4, 6, and 8 h as above, and Ang-2 mRNA levels were quantified by real-time quantitative PCR and normalized against GAPDH (21). The half-life of Ang-2 mRNA was calculated using the Sigmaplot software (SPSS, Chicago, IL).

IHC and Image Analysis. IHC was performed using the Vectastain ABC kit as described by the manufacturer (Vector, Burlingame, CA). All primary antibodies, rat antimouse CD31 (1:200; Pharmigen, San Diego, CA), mouse antihuman CD31 (1:30; Dako, Carpinteria, CA), goat anti Ang-2 (1:60; Santa Cruz Biotechnology, Santa Cruz, CA), Cy3-labeled mouse anti-α-SMA subunit (1:1200; Sigma) were incubated on sample sections for 1 h. CD31 staining density and vessel diameter were analyzed using Image-Pro Plus 4.1 software (Media Cybernetics). Immunofluorescent double staining was performed as described previously (16). The avidin-labeled Texas Red and 7-amino-4-methylcoumarin-3-acetic acid were purchased from Vector.

LCM. LCM was performed with the μCUT Laser-MicroBeam System (SL Microtest, Jena, Germany). LCM was performed as previously described (23), implementing minor modifications suggested by the manufacturer. RNA was isolated by Micro RNA Isolation kit (Refs. 23, 24; Stratagene, La Jolla, CA). IHC-assisted LCM (immuno-LCM) of endothelial cells was performed as described by others (24, 25) using CD31 rapid IHC staining with the avidin-biotin complex method.

Statistical Analysis. Data analysis was performed using SPSS statistics software package (SPSS). Statistical significance was determined by the two-tailed Student's t test. $P < 0.05$ was used for significance. The data were shown as mean $\pm$ SE or mean $\pm$ SD, as described in figure legends.

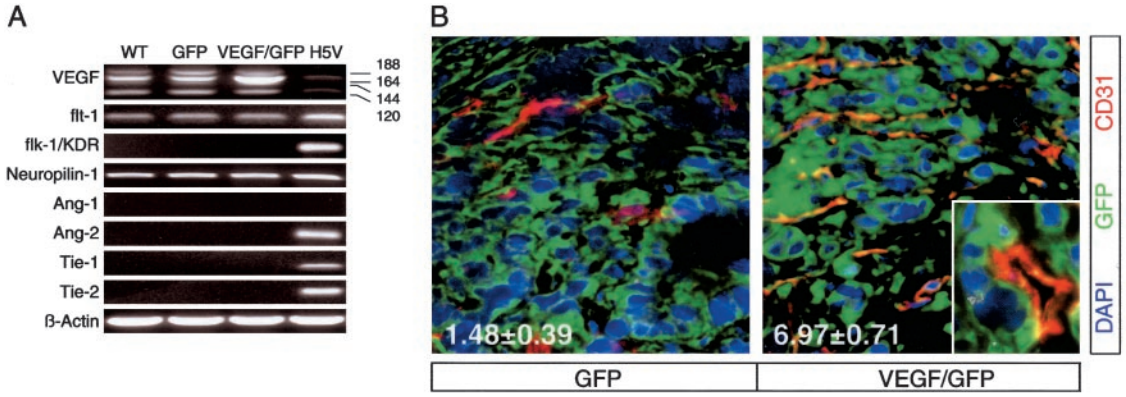

Fig. 1. A mouse model to study VEGF-induced angiogenesis in ovarian cancer. *A*, wild-type (WT) ID8 cells express three major murine VEGF isoforms, as well as VEGF receptor-1/flt-1 and coreceptor neuropilin-1 but not Angs or their receptors. Control murine immortalized endothelial cell line H5V expresses Ang-2, Tie-1, and Tie-2 but not Ang-1. *B*, a remarkably higher density of CD31-positive capillaries (*red:* CD31-positive capillary, Texas Red; *green:* GFP-positive tumor cell; *blue:* 4′,6-diamidino-2-phenylindole) is seen in a typical VEGF/GFP tumor as compared with the control GFP tumor. Numbers indicate the relative density (mean ± SE) of CD31-positive capillaries in tumor islets, as assessed by computer-aided image analysis. Capillary density is significantly higher in VEGF/GFP tumors than in control GFP tumors ($P < 0.05$).

RESULTS

A Mouse Model to Study VEGF-induced Angiogenesis in Ovarian Cancer. A murine ovarian cancer angiogenesis model induced by overexpression of VEGF164 (16) was used in this study. To test whether this model is suitable for investigating the mechanisms implicated in the regulation of Ang-2 in host stroma endothelial cells by tumor-derived VEGF, we first examined the expression *in vitro* of VEGF, Angs, as well as their receptors in ID8 epithelial ovarian cancer cells (Fig. 1*A*). It is noteworthy that ID8 cells do not express Angs or their receptors and will therefore be a most unlikely source of Ang production (Fig. 1*A*). As previously described (16), tumor-derived VEGF overexpression significantly enhanced tumor angiogenesis and accelerated tumor growth *in vivo*. Tumors overexpressing VEGF164 exhibited a significantly higher density of capillaries as compared with control tumors ($P < 0.05$; Fig. 1*B*). In addition, we analyzed molecular profiling of genes implicated in angiogenesis in the whole tumor specimens from this model, including VEGF isoforms VEGF120, VEGF164 and VEGF188; the VEGFR-1 flt-1; the VEGFR-2 flk-1/KDR; the VEGF164 coreceptor neuropilin-1; as well as CD31, by quantitative real-time RT-PCR. VEGF164 was overexpressed in VEGF164/GFP tumors as 3.5-fold compared with the GFP tumors, whereas other VEGF isoforms were not significantly different. All angiogenesis-associated genes tested were up-regulated in VEGF/GFP tumors as expected (data not shown). CD31 and VEGFR-2 flk-1/KDR levels in VEGF164/GFP tumors were 3.23- and 1.55-fold higher, respectively, compared with GFP tumors.

Ang-2 Expression and Ang-2/Tie Ratio Are Significantly Increased in VEGF-overexpressing Tumors. We quantified the absolute mRNA copy numbers of Ang-1, Ang-2, and Tie-2 in VEGF-overexpressing and control tumors by quantitative real-time RT-PCR. All following gene expression values are in numbers of gene copies/10,000 copies of GAPDH. Expression of Ang-1 was not significantly different between VEGF-overexpressing tumors (22.7 ± 6.5) and control tumors (14.7 ± 4.3; $P = 0.334$; Fig. 2*A*). Expression of Ang-2 was significantly up-regulated in VEGF-overexpressing tumors (23.1 ± 6.9) as compared with control tumors (5.3 ± 2.5; $P = 0.041$; Fig. 2*B*). The increased fold (4.40-fold) of Ang-2 was higher than that of the endothelial cells marker, CD31 (3.23-flod). Expression of Tie-2

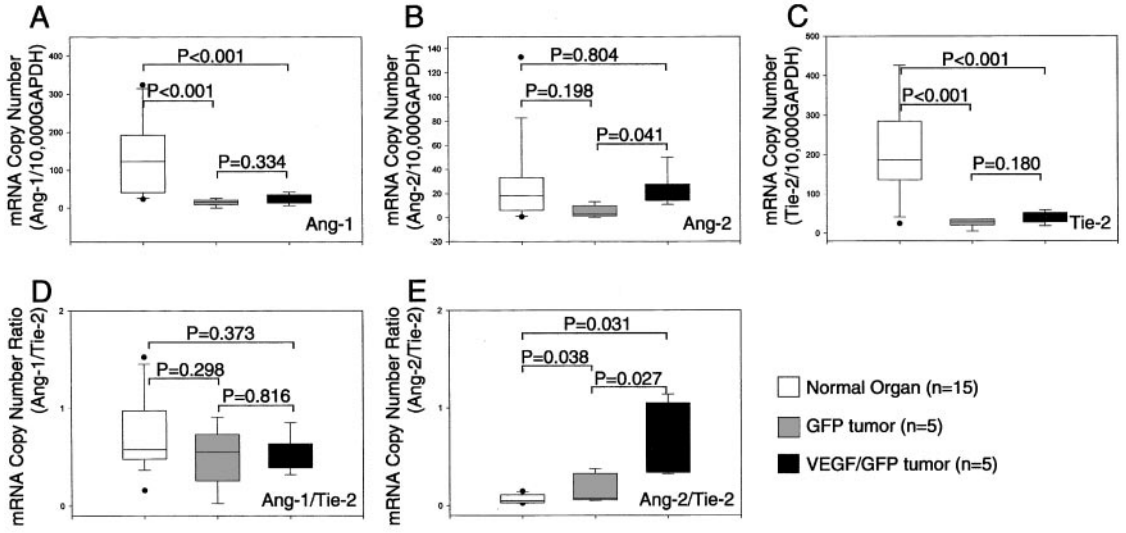

Fig. 2. Ang-2 expression and Ang-2/Tie ratio are significantly increased in VEGF-overexpressing tumors. The absolute mRNA copy numbers of Ang-1, Ang-2, and Tie-2 in tumors and 15 normal mouse tissues were quantified by a real-time RT-PCR strategy described in "Materials and Methods." *A–C*, mRNA copy numbers of Ang-1 (*A*), Ang-2 (*B*), and Tie-2 (*C*) in normal organs as well as GFP and VEGF/GFP tumors. *D* and *E*, ratios of mRNA copy number of Ang-1/Tie-2 (*D*) and Ang-2/Tie-2 (*E*) in normal organs and tumors. All gene expression values are in numbers of gene copies/10,000 copies of GAPDH.

Table 2 *Expression of Angs/Tie-2 system in normal organs and ID8 tumors mRNA copy number (target gene/10,000 GAPDH)*

	Spleen ($n = 8$)	Heart ($n = 6$)	Liver ($n = 11$)	Kidney ($n = 6$)	GFP tumor ($n = 5$)	VEGF/GFP tumor ($n = 5$)
Ang-1	147.57 ± 28.08	314.60 ± 214.05	25.30 ± 17.55	98.54 ± 26.71	14.70 ± 9.53	22.67 ± 14.46
Ang-2	19.96 ± 9.86	8.08 ± 3.28	5.84 ± 2.64	19.55 ± 4.94	5.26 ± 5.50	23.15 ± 5.51
Tie-2	132.45 ± 35.47	288.36 ± 177.64	222.03 ± 98.03	183.40 ± 70.58	25.54 ± 12.53	38.80 ± 15.84

in VEGF-overexpressing tumors (38.8 ± 7.0) was not significantly different from control tumors (25.5 ± 5.6; $P = 0.180$; Fig. 2*C*).

Because Ang-1 and Ang-2 compete for binding to Tie-2 and their molar ratio might determine the balance of Angs/Tie-2 system (26). Next, we computed the ratios of Ang-1 to Tie-2 (Ang-1/Tie-2) and Ang-2 to Tie-2 (Ang-2/Tie-2) mRNA copy numbers. It was found that the Ang-1/Tie-2 ratio was not significantly different between VEGF-overexpressing tumors and control tumors ($P = 0.816$; Fig. 2*D*). However, the Ang-2/Tie-2 ratio was significantly higher in VEGF-overexpressing tumors (0.649 ± 0.397) as compared with control tumors (0.175 ± 0.156, $P = 0.027$; Fig. 2*E*). The above results collectively show that tumor angiogenesis triggered by VEGF is associated with significantly increased expression of Ang-2, as well as a dramatic increase of Ang-2/Tie-2 but not Ang-1/Tie-2 ratio.

To gain more insight on the alterations of the Angs system associated with malignancy, we examined the expression of Ang-1, Ang-2, and Tie-2 in 15 normal organs, including spleen, heart, kidney, liver, ovary, bladder, nasal-associated lymph tissue, colon, stomach, uterus, muscle, eye, fat, tongue, and brain by quantitative real-time RT-PCR. A marked variability was noted in the expression of Ang-1, Ang-2, and Tie-2 in normal organs (Table 2). Overall, normal organs expressed significantly higher Ang-1 and Tie-2 levels compared with tumors (both $P < 0.001$; Fig. 2, *A* and *C*). Although several organs expressed markedly lower levels of Ang-2 than tumors, averaged Ang-2 levels in normal organs were not significantly different from those detected in tumors (Fig. 2*B*). Relatively high Ang-2 levels were detected in kidney and spleen (Table 2). The Ang-2/Tie-2 ratio was significantly higher in tumors as compared with average normal organs ($P < 0.05$), and the highest levels were seen in VEGF-overexpressing tumors ($P = 0.027$; Fig. 2*E*), whereas the Ang-1/Tie-2 ratio was not significantly different between tumors and normal organs (all $P > 0.05$; Fig. 2*D*). These results collectively show that malignant angiogenesis is characterized by an increased Ang-2/Tie-2 ratio compared with normal organs and that VEGF overexpression by the tumor is associated with an additional increase in the Ang-2/Tie-2 ratio.

Ang-2 Is Up-Regulated in Stroma Endothelial Cells *in Vivo*. We next sought to identify the cell type of origin of Ang-2 *in vivo* in ID8 tumors. By IHC, Ang-2 was immunolocalized to the vessels located in the stroma among tumor islets (Fig. 3*A*), as well as the stroma connecting tumors to the underlying skeletal muscles. Double immunofluorescent staining revealed that Ang-2 was exclusively expressed in CD31-positive endothelial cells (Fig. 3*B*) but not in α-SMA-positive pericytes surrounding tumor-associated vessels (Fig. 3*C*). No immunoreactive Ang-2 was detected in ID8 tumor cells.

To assess whether the observed increase in Ang-2 *in vivo* in VEGF-overexpressing tumors was related to an increase in the endothelial mass alone or also to up-regulation of Ang-2 in individual endothelial cells, we quantified Ang-2 in microdissected endothelial cells. A highly pure population of CD31-positive endothelial cells was procured by immuno-LCM from tumor stroma (Fig. 3*D*). The expression of Ang-2 in microdissected endothelial cells was confirmed by regular RT-PCR (Fig. 3*E*). Quantitative real-time RT-PCR revealed that Ang-2 expression was 4.6-fold higher ($P < 0.05$) in endothelial cells from VEGF-overexpressing tumors compared with control tumors (Fig. 3*F*). Because the only difference between these two tumors was the amount of VEGF released by tumor cells, we hypothesized that tumor-derived VEGF up-regulated Ang-2 expression in individual endothelial cells *in vivo*.

VEGF Increases Ang-2 Transcription in Cultured Endothelial Cells via KDR. To investigate whether tumor-derived VEGF can directly regulate the expression of Ang-2 in endothelial cells, we treated cultured HUVECs and immortalized murine endothelial H5V cells with CM from VEGF/GFP and GFP-transfected ID8 cells. HUVECs incubated with CM from VEGF/GFP ID8 cells expressed significantly higher levels of Ang-2 compared with cells incubated with CM from control GFP ID8 cells (Fig. 4*A*). Furthermore, CM from VEGF/GFP ID8 cells induced a markedly higher up-regulation of Ang-2 mRNA levels in H5V cells compared with CM from GFP ID8 cells. This effect could be entirely abrogated by the selective tyrosine kinase inhibitor SU1498 (27), which specifically inhibits VEGFR-2-dependent activation (Fig. 4*B*). To additionally test

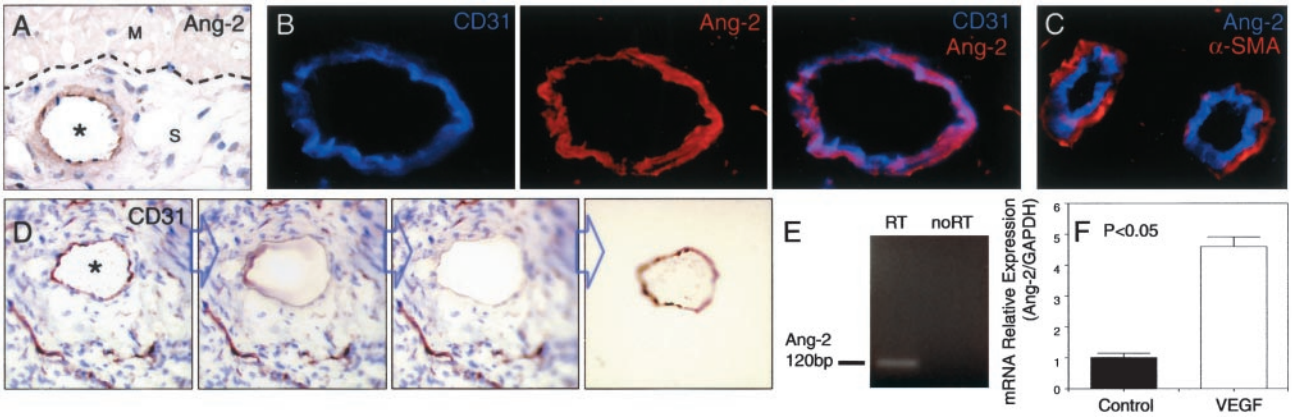

Fig. 3. Tumor-derived VEGF up-regulates Ang-2 expression in individual stroma endothelial cells *in vivo*. *A*, Ang-2 is expressed in blood vessels of the stroma located between tumor and adjacent skeletal muscles. M: skeletal muscle, S: stroma, Star: vessel. *B*, Ang-2 (*red*, Texas Red) is expressed in CD31-positive endothelial cells (*blue*, AMCA). *C*, Ang-2 (*blue*, AMCA) is absent in α-SMA-positive pericytes (*red*, Cy-3). *D*, microdissection of CD31-positive endothelial cells from the tumor stroma by LCM. *Star:* CD31-positive vessel. *E*, Ang-2 is detected by regular RT-PCR in total RNA extracted from endothelial cells procured by LCM. A single and clear band representing Ang-2 is noted at ~120 bp. *F*, real-time RT-PCR performed on microdissected endothelial cells reveals significantly higher levels of Ang-2 in VEGF/GFP tumors compared with control GFP tumors. Data are shown as mean ± SE.

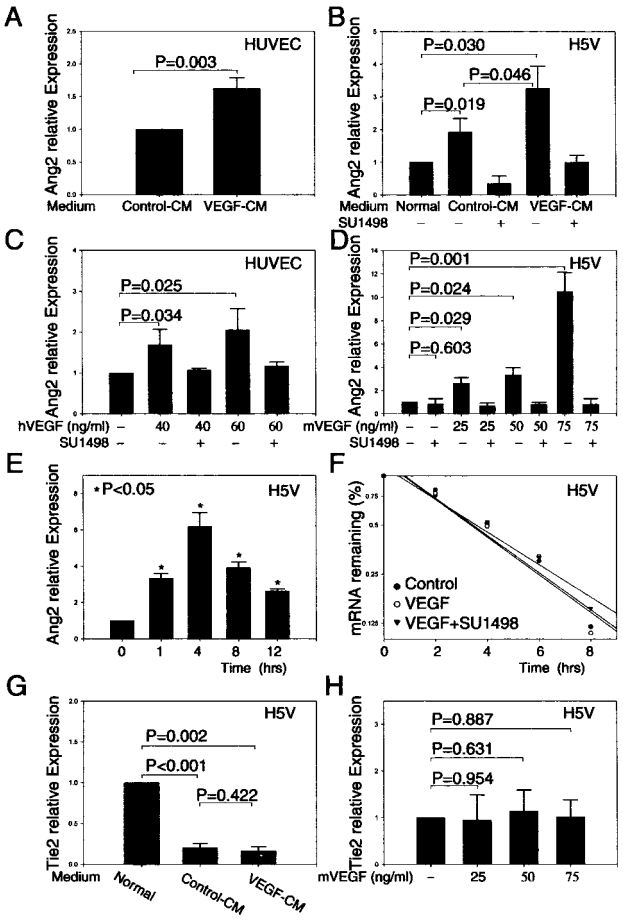

Fig. 4. VEGF increases Ang-2 transcription in cultured endothelial cells via KDR. mRNA level of Ang-2 or Tie-2 in cultured endothelial cells was quantitated by real-time RT-PCR. *A*, HUVECs were cultured in CM from GFP- (control-CM) or VEGF/GFP-transfected (VEGF-CM) ID8 cells for 6 h. *B*, H5V cells were cultured in regular media (control), control-CM, or VEGF-CM with or without SU1498 for 6 h. *C*, HUVEC cells were treated with human VEGF165 with or without SU1498 (15 μM) for 6 h. *D*, H5V cells were treated with murine VEGF164 with or without the presence of VEGFR-2 inhibitor SU1498 (15 μM) for 6 h. *E*, H5V cells were treated with murine VEGF164 for 1–12 h. Ang-2 mRNA is up-regulated by VEGF in a time-dependent manner. *F*, VEGF or VEGF plus SU1948 treatment does not significantly affect the mRNA stability of Ang-2 in H5V. Log-linear regression lines of mRNA degradation of Ang-2 are shown. *G*, H5V cells were cultured in regular media (control), in control-CM, or VEGF-CM for 6 h. *H*, H5V cells were treated with murine VEGF164 for 6 h. All experiments were repeated at least three times. Data are shown as mean ± SD.

whether VEGF can directly induce Ang-2 expression in endothelial cells and to identify the VEGF receptor(s) mediating this process, we treated HUVECs and H5V cells with recombinant human VEGF165 and murine VEGF164, respectively. Ang-2 mRNA levels were up-regulated by species-specific recombinant VEGF in a dose-dependent and time-dependent manner (Fig. 4, *C–E*); moreover, such effect of VEGF could be abolished by SU1498 (Fig. 4, *C* and *D*). VEGF or VEGF plus SU1498 treatment did not significantly affect the stability of Ang-2 mRNA in H5V cells (Fig. 4*F*), indicating that the effect on Ang-2 expression was primarily because of transcriptional activation. These results indicate that VEGF can directly up-regulate Ang-2 in endothelium through a paracrine mechanism via VEGFR-2/flk-1/KDR.

To examine whether tumor VEGF also affects the expression of Tie-2 in endothelial cells, Tie-2 mRNA expression was quantified in the same samples as above. CM from both the VEGF/GFP and control GFP ID8 cells significantly decreased Tie-2 mRNA expression in endothelial cells, but there was no significant difference in their effect (Fig. 4*G*). Furthermore, recombinant VEGF did not affect the expression of Tie-2 in H5V cells. These data indicate that in contrast to Ang-2, Tie-2 expression is not dependent on VEGF but is regulated by alternate paracrine factors released by tumor cells.

Ang-2 and VEGF mRNA Levels Correlate in Human Ovarian Carcinoma. To investigate whether a correlation exists between the expression of VEGF, Ang-1, Ang-2, and Tie-2 in human ovarian carcinoma, we examined their mRNA level in 52 human ovarian carcinoma specimens. A significant correlation was only observed between Ang-2 and VEGF ($P < 0.01$; Fig. 5*B*) but not between VEGF and Ang-1 ($P = 0.974$) or Tie-2 ($P = 0.728$) in these specimens (Fig. 5, *A* and *C*).

Ang-2 Is Primarily Expressed in Stroma Endothelial Cells in Human Ovarian Carcinoma. We next sought to characterize the expression of Ang-2 in human ovarian carcinoma. Using IHC, we found that Ang-2 was highly expressed in endothelial cells of large and medium caliber blood vessels in human ovarian carcinoma samples (Fig. 6*A*). Ang-2-positive blood vessels were predominantly localized in tumor stroma. In agreement with recent reports that tumor cells may express Ang-2 (28–30), Ang-2-positive tumor cells were detected in tumor islets of 12% samples analyzed (Fig. 6*B*), and double IHC staining confirmed the coexpression of Ang-2 and cytokeratin, indicating that select tumor cells may produce Ang-2 *in vivo* (Fig. 6*C*). To confirm that tumor cells indeed express Ang-2, we examined 36 human cancer cell lines and detected Ang-2 mRNA clearly in 7 of 14 ovarian, 9 of 13 colon, 3 of 5 breast, and 3 other tumor cell lines (Fig. 6*D*). However, quantitative real-time RT-PCR revealed that only 4 of 36 cell lines, including ovarian cancer line OVCAR5, had Ang-2 mRNA levels comparable with the average Ang-2 mRNA levels observed in human tumor samples, whereas the remainder lines displayed 100-1000-fold lower levels of Ang-2 mRNA compared with the average levels detected in human tumor samples (Fig. 6*E*). To additionally address the origin of Ang-2 pro-

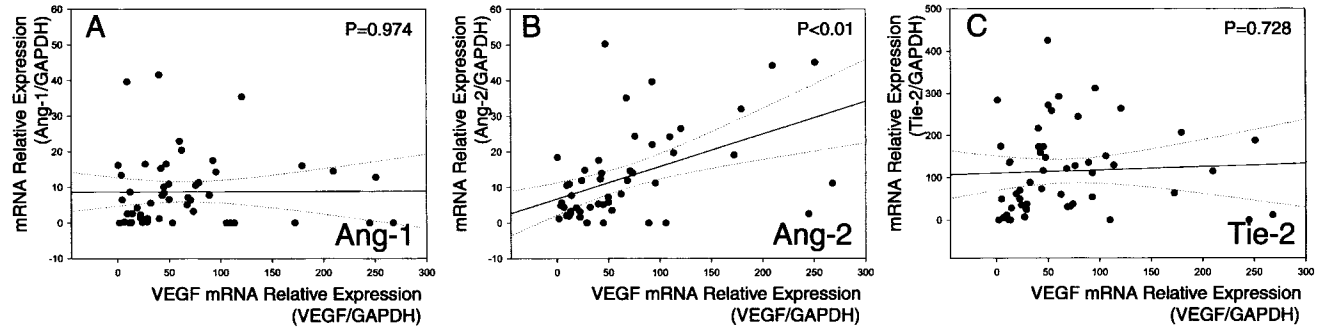

Fig. 5. Ang-2 and VEGF mRNA levels correlate in human ovarian carcinoma. mRNA was isolated from 52 human ovarian carcinoma samples and quantitated by real-time RT-PCR. Significant correlation is noted between the mRNA levels of Ang-2 and VEGF ($P < 0.01$; *B*) but not between VEGF and Ang-1 ($P = 0.974$; *A*) or Tie-2 ($P = 0.728$; *C*).

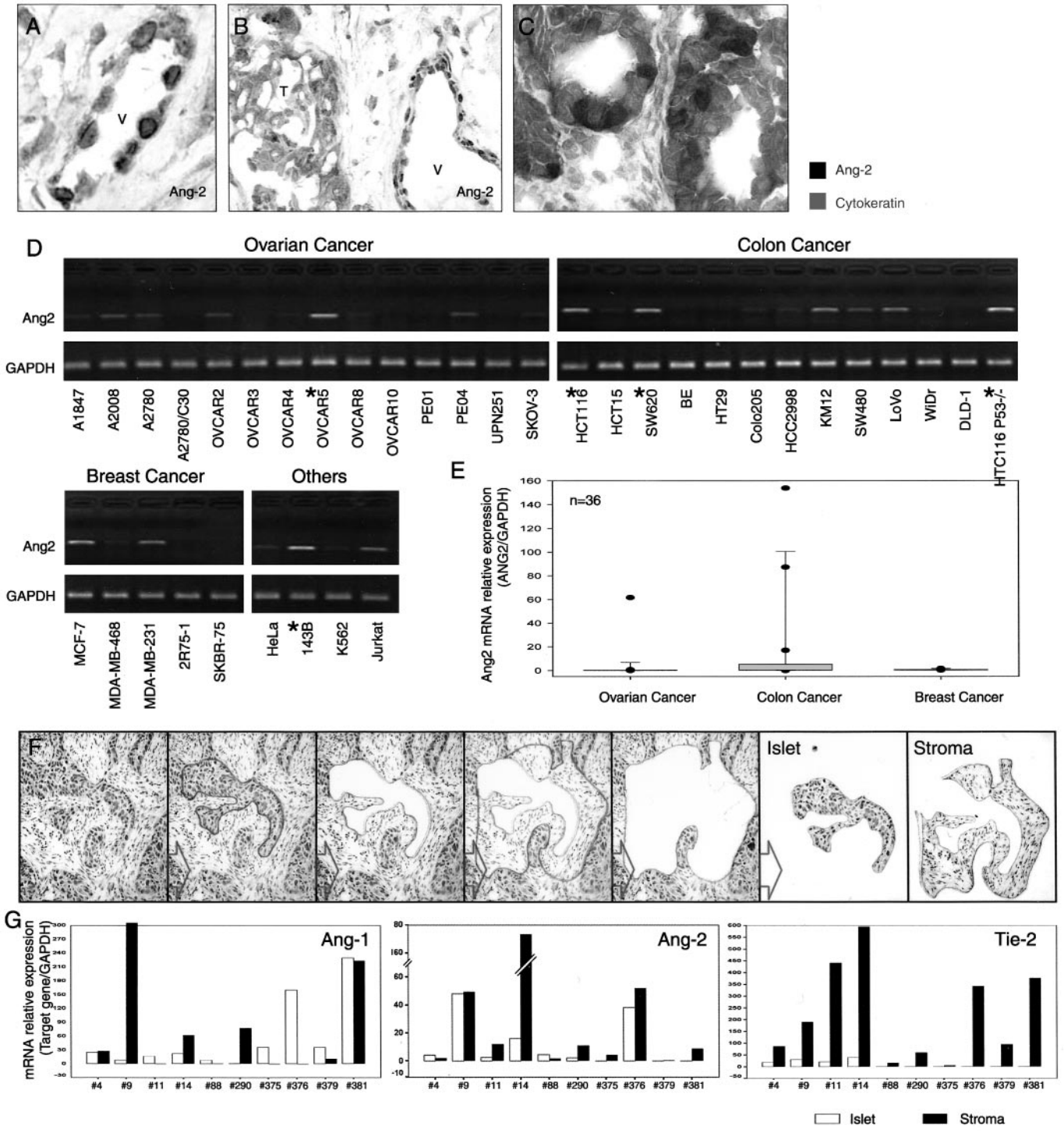

Fig. 6. Ang-2 is primarily expressed in stroma endothelial cells in human ovarian carcinoma. *A–C*, immunohistochemical staining of Ang-2 in human ovarian carcinoma specimens. Ang-2 is highly expressed by endothelial cells in the stroma (*A* and *B*) as well as the tumor islets of 12% patients (*B*). Double staining shows Ang-2 (*red*, AP) coexpressed in cytokeratin-positive tumor cells (*brown*, 3,3′-diaminobenzidine) in select specimens (*C*). V: vessel, T: tumor islet. *D*, mRNA expression of Ang-2 in human cancer cell lines studied by RT-PCR. Ang-2 mRNA is detected clearly in ovarian (7 of 14), colon (9 of 13), breast (3 of 5), and other (3 of 4) cancer cell lines cultured *in vitro*. *E*, quantitation of Ang-2 mRNA in human cancer cell lines by real-time RT-PCR. Only 4 of 36 cell lines exhibit high levels of Ang-2 (comparable with the average Ang-2 mRNA levels detected in human tumor specimens), whereas 11 of 36 cell lines show Ang-2 levels at ~1/100–1/1000 of the average level detected in human tumor samples. *F* and *G*, tumor islets and surrounding stroma were microdissected from 10 advanced stage ovarian tumors by LCM (*F*). mRNA levels of Ang-1, Ang-2, and Tie-2 in each pair of the microdissected islet and stroma were quantitated by real-time RT-PCR. Ang-1 mRNA level is higher in 4 of 10 stroma samples and lower in 6 of 10 stroma as compared with matched islet samples; Ang-2 is higher in 8 of 10 stroma and slightly lower in 2 of 10 stroma *versus* matched islet samples, and Tie-2 is significantly higher in 10 of 10 stroma *versus* matched islet samples.

duction in human ovarian carcinoma, 10 stage III ovarian carcinoma samples were subject to LCM to isolate tumor islets and matched surrounding stroma (Fig. 6*F*). Ang-1 mRNA level was higher in 3 of 10 stroma specimens, lower in 5 of 10 stroma specimens, and similar in 2 of 10 as compared with the matched tumor islet specimens (Fig. 6*G*). However, Ang-2 mRNA level was higher in 7 of 10 stroma specimens, lower in 2 of 10 stroma specimens, and similar in 1 of 10 stroma specimens *versus* the matched tumor islet specimens (Fig. 6*G*),

suggesting that Ang-2 is primarily produced by stroma-derived host cells. Interestingly, Tie-2 mRNA levels were significantly higher in stroma as compared with the matched islets in all 10 samples tested (Fig. 6*G*). The above data collectively indicate that in human ovarian carcinoma Ang-2 is primarily expressed in stromal vascular endothelial cells but not tumor cells.

Up-Regulation of Ang-2 in Endothelium Induced by Tumor-derived VEGF Is Associated with Pericyte Loss and Vascular Instability. Tumor microvasculature displays immature features, exhibiting a discontinuous or entirely absent pericyte layer (31, 32). The mechanisms underlying the disruption of pericyte layer are not understood, but recent evidence has implicated a cooperation between VEGF and Ang-2 (2, 33). To investigate how VEGF overexpression and consequent up-regulation of Ang-2 in stroma endothelial cells affect pericytes *in vivo*, we studied the prevalence of pericytes in the vasculature surrounding tumors. α-SMA was used as a marker for the identification of pericytes by immunostaining. We first examined host vasculature associated with tumors but at relatively distant sites, *i.e.*, within the skeletal muscles underlying flank tumors. Large and medium caliber vessels residing in skeletal muscles next to GFP tumors were surrounded by a continuous layer of α-SMA-positive pericytes. However, vessels examined in skeletal muscles adjacent to flank tumors overexpressing VEGF exhibited a more destabilized phenotype, with a disarrayed pericyte layer (Fig. 7*C*). Next, we examined the host vasculature closer to tumors, *i.e.*, located in the stroma connecting tumor nodules adjacent to skeletal muscles. A great number of large vessels could be seen in this location (Fig. 7*A*). Although destabilized features with disorganization of the pericyte layer was observed in both tumor groups, pericyte loss was markedly more prominent—and even complete in some cases—in the stroma supporting VEGF/GFP tumors compared with control GFP tumors (Fig. 7*E*). The percentage of blood vessels lacking $>$50% of the pericyte layer was significantly higher in the VEGF164/GFP group ($72.1 \pm 5.6\%$) than the control GFP group ($39.4 \pm 7.9\%$; $P < 0.05$; Fig. 7*B*). These differences were specific only for large and medium caliber vessels. In both tumor types, capillaries located within skeletal muscles (Fig. 7*C*) the stroma (Fig. 7*E*) or within the tumors (Fig. 7*D*) were barely covered by α-SMA-positive pericytes, in keeping with previous reports that pericytes are absent in capillaries (32). These data collectively provide the evidence that tumor VEGF overexpression is associated with distant paracrine effects on the supporting host vasculature, inducing a destabilized phenotype with loss of the pericyte layer.

To investigate whether similar vascular instability also occurs in human ovarian carcinoma, we examined 51 human ovarian carcinoma samples in serial sections using IHC for α-SMA and CD31. The distribution of pericytes in human samples was very similar to what was observed in the mouse model. A remarkable loss of pericytes was observed in 25.5% (13 of 51) of ovarian carcinoma specimens. Large and medium caliber vessels were detected within tumor stroma, which displayed a severely disrupted pericyte layer, with some tumors entirely lacking pericytes around stroma vessels (Fig. 7*G*).

DISCUSSION

Central to the successful development of tumor neovasculature is the remodeling of preexisting vessels in host tissues surrounding the growing tumor mass. Cooperation between VEGF and the Ang system is considered to be critical in this context. In this study, we showed that endothelial cells of tumor-associated host vasculature are the primary source of Ang-2 in tumors and demonstrated that the coordinated expression of VEGF and Ang-2 in the context of tumor angiogenesis is because of a paracrine mechanism mediated by tumor-derived VEGF *in vivo*. In addition, the *in vitro* experiments demonstrated that this effect is mediated via VEGFR-2/flk-2/KDR, which is dose- and time-dependent and resulted from transcriptional activation rather than enhanced mRNA stability. In agreement with the demonstrated interaction between VEGF and Ang-2 in the mouse model, we found a significant, positive correlation between the two molecules in many human ovarian carcinoma specimens.

Remodeling of the tumor-associated host vasculature entails structural destabilization with disruption of the pericyte mantle (31, 32). The important role of Ang-2 in inducing vascular stability in the context of tumor angiogenesis has been suggested by histopathological observations (29) and by a xenograft gastric cancer model overexpressing Ang-2 (33). Importantly, the angiogenic response requires concomitant activity by Ang-2 and VEGF because Ang-2 alone may result in vessel regression (9, 10). In keeping with these reports, we found that VEGF overexpression in the tumor led to increased vasculature destabilization in surrounding host tissues. A significantly higher prevalence of pericyte loss was seen in the stroma surrounding VEGF-overexpressing tumors compared with control tumors. In addition, these vascular abnormalities were more extensive in host tissues associated with VEGF-overexpressing tumors, reaching into the adjacent flank muscles, whereas they could not be detected in muscle underlying control tumors. Importantly, these effects were associated with a concomitant up-regulation of Ang-2 both within the tumor in general, as well as within tumor endothelium of host stroma.

Thus far the mechanism by which Ang-2 promotes the disruption of the pericyte layer remains elusive. However, evidence indicates that Ang-2 may be a natural antagonist of Ang-1 and that pericyte loss induced by Ang-2 may be the result of competitive inhibition of Ang-1 binding to the shared receptor Tie-2 (2, 8). Because the balance between Ang-1 and Ang-2 appears to hold the switch to vascular remodeling, we used quantitative real-time RT-PCR to measure the absolute copy numbers of Ang-1, Ang-2, and Tie-2 in the mouse tumor model. VEGF overexpression was associated with a significant increase in Ang-2 but not Ang-1 or Tie-2 copy numbers. As a result, in tumors with VEGF overexpression, the mRNA copy number ratio of Ang-2/Tie-2 is significantly higher than control tumor. This was associated with increased vascular instability, supporting the notion that the dynamic balance between Ang-1, Ang-2, and Tie-2, rather than the expression level of individual genes, may be critical for the regulation of vascular stability.

The effect of Ang-2 on tumor growth has been extensively studied (28, 33–36), but the reported results have not been consistent. Importantly, most of the above studies are based on the effects of exogenous Ang-2 or overexpression of Ang-2 by tumor cells (28, 33–36). Although at physiological concentrations Ang-2 may antagonize Ang-1 promoting vascular instability (5, 8), *in vitro* data have shown that at high concentrations Ang-2 can function as an agonist (37). Therefore, it is questionable whether tumor models examining the effects of Ang-2 overexpression *in vivo* after transfection of tumor cells can accurately recapitulate the effects of a physiological Ang-2 increase. Various reports have shown that Ang-2 may be expressed in human solid tumors (12, 28, 29, 35, 36, 38–40). Interestingly, hypoxia may up-regulate Ang-2 expression in certain cancer cell lines (29), supporting its role in promoting angiogenesis in tumors. Our data show that a small proportion of established ovarian cancer cells express Ang-2 and that *in vivo* Ang-2 mainly derives from stroma endothelial cells rather than tumor cells. Only in select cases, Ang-2 was also expressed at high levels in tumor cells. Our tumor model, therefore, accurately recapitulates molecular events occurring in human ovarian cancer, where tumor cell-derived VEGF drives the expression of Ang-2.

On the basis of our findings, an integrated model of VEGF-Ang-2

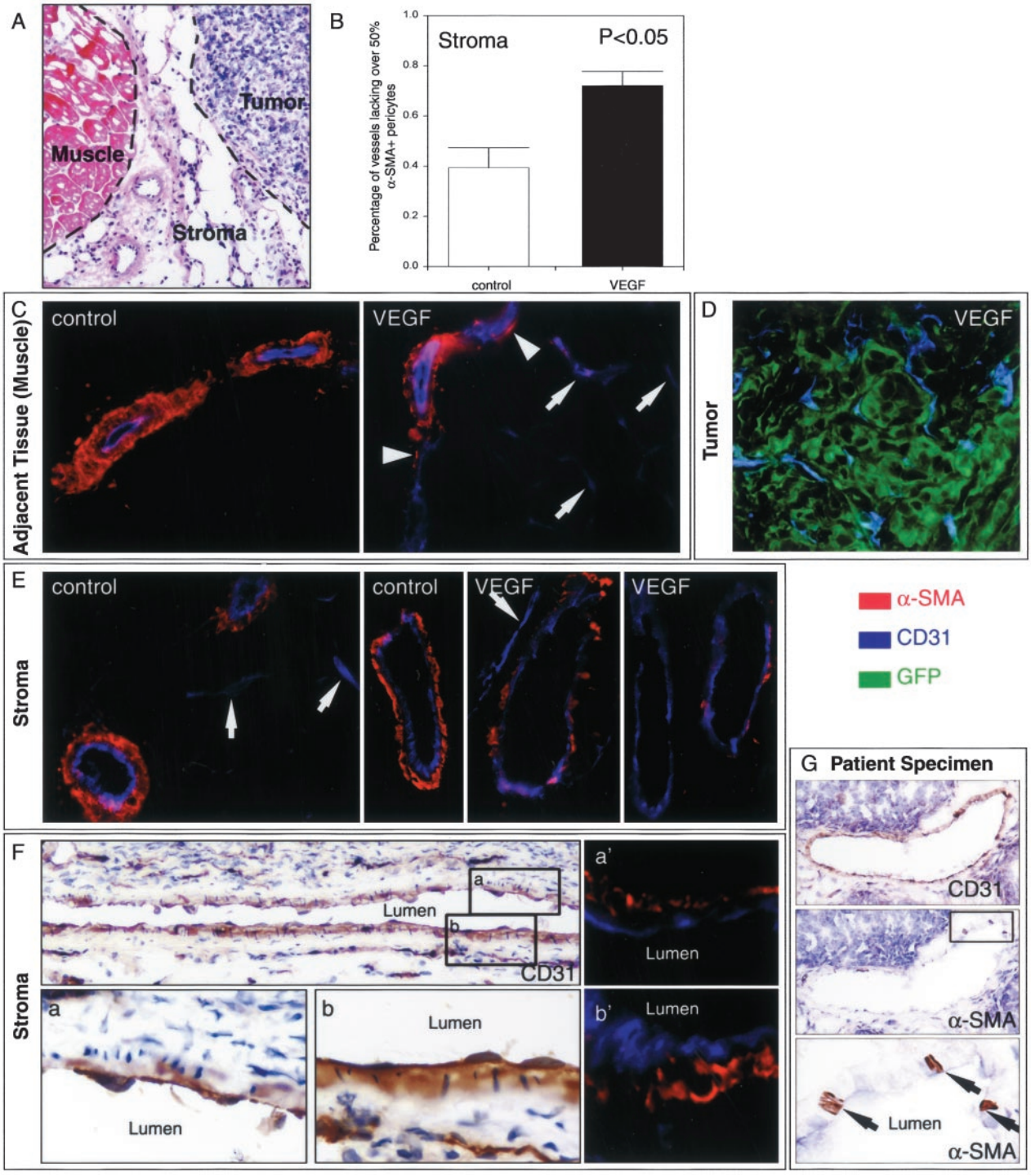

Fig. 7. Up-regulation of Ang-2 in endothelium induced by tumor-derived VEGF is associated with pericyte loss and vascular instability. *A* and *B*, summary of vascular stability in mouse tumors as assessed by pericyte immunostaining with a monoclonal antibody against α-SMA. *A*, H&E-staining depicts the three areas investigated for the distribution of pericytes (from *right to left*): tumor, surrounding stroma and adjacent skeletal muscle. *B*, quantitative evaluation of the pericyte layer in stroma vessels. A significantly larger fraction of stroma vessels lack >50% of the pericyte layer in VEGF-overexpressing tumors compared with control tumors. Data are shown as mean ± SE. *C–F*, pericyte detection in mouse tumors. *C*, in skeletal muscles underlying control GFP tumors, medium caliber vessels are surrounded by a continuous layer of α-SMA-positive pericytes, whereas in skeletal muscles underlying VEGF164/GFP tumors, the pericyte layer is disrupted (*arrowhead*). α-SMA-negative capillaries are noted (*arrows*). *D*, abundant α-SMA-negative capillaries are seen in a tumor islet in VEGF-overexpressing tumors (or control tumors, data not shown). *E*, in stroma surrounding control GFP tumors, large and medium caliber vessels are surrounded by a continuous layer of pericytes. *Arrows* show capillaries. In stroma surrounding VEGF164/GFP tumors, large and medium caliber vessels exhibit disrupted α-SMA-positive pericyte layer or complete loss of pericytes. *Arrows* show capillaries. *F*, CD31 immunostaining depicting a longitudinal section of a medium caliber blood vessel in the stroma of a VEGF164/GFP tumor. *a* and *b* are high-power fields of two different loci on this vessel. Endothelial cell crowding is noted with an inner layer of longitudinally oriented cells and an outer layer of CD31-positive cuboidal cells with nuclei orientated perpendicularly to the vessel axis. *a'* and *b'* are areas matched to *a* and *b*, respectively, from an adjacent section. Disruption of the α-SMA-positive pericyte layer is noted in these areas. *G*, pericyte detection in human ovarian carcinoma by α-SMA immunostaining. A typical medium caliber vessel is shown in the stroma of a human ovarian carcinoma sample. CD31 immunostaining defines the endothelial cell layer (*top*). The pericyte layer is almost entirely lost, as assessed by α-SMA immunostaining of an adjacent section (*middle*). Few α-SMA-positive pericytes are seen in a high-power field (*bottom*). *Blue* (AMCA) = CD31; *red* (Cy-3) = α-SMA; *green* (GFP) = tumor cells; *brown* = 3,3′-diaminobenzidine.

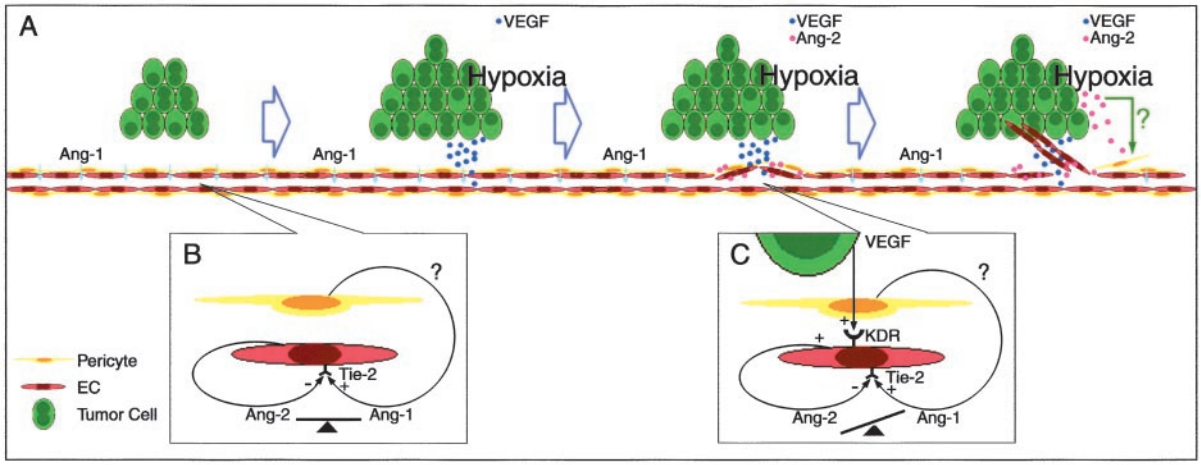

Fig. 8. Proposed model of enhanced tumor angiogenesis via VEGF-induced up-regulation of Ang-2 in host endothelium. *A*, in endothelial cells of the normal host tissues, the balance of Ang-1 and Ang-2 in the microenvironment affords microvasculature stability. Growing nearby tumors undergo hypoxia, up-regulating VEGF, which induces in a paracrine fashion up-regulation of Ang-2 in the endothelium of adjacent host vessels. Increased Ang-2 secretion by the endothelium acts to perturb the preexisting interactions between Ang-1 and endothelial Tie-2, resulting in loss of pericytes and destabilization of the vascular walls, a *sine qua non* for the support of angiogenesis in the developing tumor. *B*, the hypothesized molecular events underlying vascular stability are depicted. Ang-1 and Ang-2 compete for binding to Tie-2. Excess of Ang-1, partly derived from the pericyte layer, ensures vascular integrity. *C*, tumor-derived VEGF up-regulates endothelial Ang-2 in proximal host vessels via VEGFR2/flk-1/KDR, which in an autocrine fashion results in competitive perturbance of the Ang-1/Tie interactions.

cooperation could be hypothesized (Fig. 8). In this model, normal host tissues exhibit stable microvasculature, which is afforded by excess Ang-1 production in the microenvironment, partly derived from the pericyte layer (41). Tumor-derived VEGF produced in response to hypoxia, growth factors, and/or genetic alterations (42) induces—via VEGFR-2/KDR—up-regulation of Ang-2 in the endothelium of host vessels adjacent to the tumor. Increased Ang-2 secretion by the endothelium acts in an autocrine manner to perturb the preexisting interactions between Ang-1 and endothelial Tie-2. This results in loss of pericytes and destabilization of the vascular walls, according to current views (2, 7). Therefore, VEGF, in its function as a master regulator of the angiogenic switch, promotes angiogenesis through multiple and complementary mechanisms. Not only does it promotes the recruitment and proliferation of endothelial cells and their precursors within the tumor, but it also furnishes nearby host vessels the necessary plasticity to support angiogenesis in developing tumors. The fact that VEGF can up-regulate flk-1/KDR (43) and neuropilin-1 (44) in cultured endothelial cells provides additional evidence of the complexity of the molecular events constituting the angiogenic switch.

Many questions still remain to be addressed concerning the interactions of VEGF and Ang-2 in the context of tumor angiogenesis. For example, the role of other VEGF isoforms in this process needs to be investigated because different isoforms may play distinct roles in tumor angiogenesis (45, 46). Furthermore, additional tumor-derived factors may contribute to the destabilization of host vasculature through the down-regulation of endothelial Tie-2, as our *in vitro* and *in vivo* findings suggest. In addition, we investigated these interactions during the growth of established tumors (*i.e.*, 10 weeks after tumor inoculation); whether similar mechanisms apply to the tumors at a very early stage of development is not yet known. Expression of Ang-2 before VEGF during the first weeks of tumor growth has been reported (9). Importantly, in this study, we used an ectopic mouse ovarian tumor model constructed with relatively rapidly growing tumor cells. Although widely used in preclinical studies of tumor angiogenesis, such models may not exactly replicate the cellular and molecular events characterizing human tumors (4). Tumor growth in the ectopic s.c. site may be different from orthotopic growth in the peritoneal cavity. Additional investigation under conditions better mimicking the natural environment of human ovarian tumors is therefore highly desirable. Finally, in this study, overexpression of VEGF could likewise lead to aberrant downstream activity and difficulty in data interpretations.

ACKNOWLEDGMENTS

We thank Dr. Paul F. Terranova for donating the murine ID8 cells, Dr. Warren Pear for the MigR1 vector and BOSC 23-packaging cell line, Dr. Patricia D'Amore for the VEGF164 cDNA, and Drs. Steven Johnson and Kang-Sheng Yao for the human ovarian cancer cells.

REFERENCES

1. Folkman, J. Tumor angiogenesis: therapeutic implications. N. Engl. J. Med., *285:* 1182–1186, 1971.
2. Yancopoulos, G. D., Davis, S., Gale, N. W., Rudge, J. S., Wiegand, S. J., and Holash, J. Vascular-specific growth factors and blood vessel formation. Nature (Lond.), *407:* 242–248, 2000.
3. Hanahan, D., and Folkman, J. Patterns and emerging mechanisms of the angiogenic switch during tumorigenesis. Cell, *86:* 353–364, 1996.
4. Kerbel, R. S. Tumor angiogenesis: past, present and the near future. Carcinogenesis (Lond.), *21:* 505–515, 2000.
5. Papetti, M., and Herman, I. M. Mechanisms of normal and tumor-derived angiogenesis. Am. J. Physiol. Cell Physiol., *282:* C947–C970, 2002.
6. Carmeliet, P., and Jain, R. K. Angiogenesis in cancer and other diseases. Nature (Lond.), *407:* 249–257, 2000.
7. Lauren, J., Gunji, Y., and Alitalo, K. Is angiopoietin-2 necessary for the initiation of tumor angiogenesis? Am. J. Pathol., *153:* 1333–1339, 1998.
8. Maisonpierre, P. C., Suri, C., Jones, P. F., Bartunkova, S., Wiegand, S. J., Radziejewski, C., Compton, D., McClain, J., Aldrich, T. H., Papadopoulos, N., Daly, T. J., Davis, S., Sato, T. N., and Yancopoulos, G. D. Angiopoietin-2, a natural antagonist for Tie2 that disrupts *in vivo* angiogenesis. Science (Wash. DC), *277:* 55–60, 1997.
9. Holash, J., Maisonpierre, P. C., Compton, D., Boland, P., Alexander, C. R., Zagzag, D., Yancopoulos, G. D., and Wiegand, S. J. Vessel cooption, regression, and growth in tumors mediated by angiopoietins and VEGF. Science (Wash. DC), *284:* 1994–1998, 1999.
10. Lobov, I. B., Brooks, P. C., and Lang, R. A. Angiopoietin-2 displays VEGF-dependent modulation of capillary structure and endothelial cell survival *in vivo*. Proc. Natl. Acad. Sci. USA, *99:* 11205–11210, 2002.
11. Visconti, R. P., Richardson, C. D., and Sato, T. N. Orchestration of angiogenesis and arteriovenous contribution by angiopoietins and vascular endothelial growth factor (VEGF). Proc. Natl. Acad. Sci. USA, *99:* 8219–8224, 2002.
12. Stratmann, A., Risau, W., and Plate, K. H. Cell type-specific expression of angiopoietin-1 and angiopoietin-2 suggests a role in glioblastoma angiogenesis. Am. J. Pathol., *153:* 1459–1466, 1998.
13. Vajkoczy, P., Farhadi, M., Gaumann, A., Heidenreich, R., Erber, R., Wunder, A., Tonn, J. C., Menger, M. D., and Breier, G. Microtumor growth initiates angiogenic

sprouting with simultaneous expression of VEGF, VEGF receptor-2, and angiopoietin-2. J. Clin. Investig., *109:* 777–785, 2002.
14. Mandriota, S. J., and Pepper, M. S. Regulation of angiopoietin-2 mRNA levels in bovine microvascular endothelial cells by cytokines and hypoxia. Circ. Res., *83:* 852–859, 1998.
15. Oh, H., Takagi, H., Suzuma, K., Otani, A., Matsumura, M., and Honda, Y. Hypoxia and vascular endothelial growth factor selectively up-regulate angiopoietin-2 in bovine microvascular endothelial cells. J. Biol. Chem., *274:* 15732–15739, 1999.
16. Zhang, L., Yang, N., Conejo Garcia, J. R., Mohamed, A., Benencia, F., Rubin, S. C., Allman, D., and Coukos, G. Generation of a syngeneic mouse model to study the effects of vascular endothelial growth factor in ovarian carcinoma. Am. J. Pathol., *161:* 2295–2309, 2002.
17. Garlanda, C., Parravicini, C., Sironi, M., De Rossi, M., Wainstok de Calmanovici, R., Carozzi, F., Bussolino, F., Colotta, F., Mantovani, A., and Vecchi, A. Progressive growth in immunodeficient mice and host cell recruitment by mouse endothelial cells transformed by polyoma middle-sized T antigen: implications for the pathogenesis of opportunistic vascular tumors. Proc. Natl. Acad. Sci. USA, *91:* 7291–7295, 1994.
18. Coukos, G., Makrigiannakis, A., Amin, K., Albelda, S. M., and Coutifaris, C. Platelet-endothelial cell adhesion molecule-1 is expressed by a subpopulation of human trophoblasts: a possible mechanism for trophoblast-endothelial interaction during haemochorial placentation. Mol. Hum. Reprod., *4:* 357–367, 1998.
19. Roby, K. F., Taylor, C. C., Sweetwood, J. P., Cheng, Y., Pace, J. L., Tawfik, O., Persons, D. L., Smith, P. G., and Terranova, P. F. Development of a syngeneic mouse model for events related to ovarian cancer. Carcinogenesis (Lond.), *21:* 585–591, 2000.
20. Zhang, L., Conejo-Garcia, J. R., Katsaros, D., Gimotty, P. A., Massobrio, M., Regnani, G., Makrigiannakis, A., Gray, H., Schlienger, K., Liebman, M. N., Rubin, S. C., and Coukos, G. Intratumoral T cells, recurrence, and survival in epithelial ovarian cancer. N. Engl. J. Med., *348:* 203–213, 2003.
21. Zhang, L., Conejo-Garcia, J. R., Yang, N., Huang, W., Mohamed-Hadley, A., Yao, W., Benencia, F., and Coukos, G. Different effects of glucose starvation on expression and stability of VEGF mRNA isoforms in murine ovarian cancer cells. Biochem. Biophys. Res. Commun., *292:* 860–868, 2002.
22. Zhang, L., Yang, N., Mohamed-Hadley, A., Rubin, S. C., and Coukos, G. Vector-based RNAi, a novel tool for isoform-specific knock-down of VEGF and anti-angiogenesis gene therapy of cancer. Biochem. Biophys. Res. Commun., *303:* 1169–1178, 2003.
23. Zhang, L., Yang, N., Conejo-Garcia, J. R., Katsaros, D., Mohamed-Hadley, A., Fracchioli, S., Schlienger, K., Toll, A., Levine, B., Rubin, S. C., and Coukos, G. Expression of endocrine gland-derived vascular endothelial growth factor in ovarian carcinoma. Clin. Cancer Res., *9:* 264–272, 2003.
24. Fend, F., Emmert-Buck, M. R., Chuaqui, R., Cole, K., Lee, J., Liotta, L. A., and Raffeld, M. Immuno-LCM: laser capture microdissection of immunostained frozen sections for mRNA analysis. Am. J. Pathol., *154:* 61–66, 1999.
25. Simone, N. L., Remaley, A. T., Charboneau, L., Petricoin, E. F., III, Glickman, J. W., Emmert-Buck, M. R., Fleisher, T. A., and Liotta, L. A. Sensitive immunoassay of tissue cell proteins procured by laser capture microdissection. Am. J. Pathol., *156:* 445–452, 2000.
26. Shih, S. C., Robinson, G. S., Perruzzi, C. A., Calvo, A., Desai, K., Green, J. E., Ali, I. U., Smith, L. E., and Senger, D. R. Molecular profiling of angiogenesis markers. Am. J. Pathol., *161:* 35–41, 2002.
27. Strawn, L. M., McMahon, G., App, H., Schreck, R., Kuchler, W. R., Longhi, M. P., Hui, T. H., Tang, C., Levitzki, A., Gazit, A., Chen, I., Keri, G., Orfi, L., Risau, W., Flamme, I., Ullrich, A., Hirth, K. P., and Shawver, L. K. Flk-1 as a target for tumor growth inhibition. Cancer Res., *56:* 3540–3545, 1996.
28. Tanaka, S., Mori, M., Sakamoto, Y., Makuuchi, M., Sugimachi, K., and Wands, J. R. Biologic significance of angiopoietin-2 expression in human hepatocellular carcinoma. J. Clin. Investig., *103:* 341–345, 1999.
29. Koga, K., Todaka, T., Morioka, M., Hamada, J., Kai, Y., Yano, S., Okamura, A., Takakura, N., Suda, T., and Ushio, Y. Expression of angiopoietin-2 in human glioma cells and its role for angiogenesis. Cancer Res., *61:* 6248–6254, 2001.
30. Hatanaka, H., Abe, Y., Naruke, M., Tokunaga, T., Oshika, Y., Kawakami, T., Osada, H., Nagata, J., Kamochi, J., Tsuchida, T., Kijima, H., Yamazaki, H., Inoue, H., Ueyama, Y., and Nakamura, M. Significant correlation between interleukin 10 expression and vascularization through angiopoietin/TIE2 networks in non-small cell lung cancer. Clin. Cancer Res., *7:* 1287–1292, 2001.
31. Benjamin, L. E., Golijanin, D., Itin, A., Pode, D., and Keshet, E. Selective ablation of immature blood vessels in established human tumors follows vascular endothelial growth factor withdrawal. J. Clin. Investig., *103:* 159–165, 1999.
32. Morikawa, S., Baluk, P., Kaidoh, T., Haskell, A., Jain, R. K., and McDonald, D. M. Abnormalities in pericytes on blood vessels and endothelial sprouts in tumors. Am. J. Pathol., *160:* 985–1000, 2002.
33. Etoh, T., Inoue, H., Tanaka, S., Barnard, G. F., Kitano, S., and Mori, M. Angiopoietin-2 is related to tumor angiogenesis in gastric carcinoma: possible *in vivo* regulation via induction of proteases. Cancer Res., *61:* 2145–2153, 2001.
34. Yu, Q., and Stamenkovic, I. Angiopoietin-2 is implicated in the regulation of tumor angiogenesis. Am. J. Pathol., *158:* 563–570, 2001.
35. Hawighorst, T., Skobe, M., Streit, M., Hong, Y. K., Velasco, P., Brown, L. F., Riccardi, L., Lange-Asschenfeldt, B., and Detmar, M. Activation of the tie2 receptor by angiopoietin-1 enhances tumor vessel maturation and impairs squamous cell carcinoma growth. Am. J. Pathol., *160:* 1381–1392, 2002.
36. Ahmad, S. A., Liu, W., Jung, Y. D., Fan, F., Wilson, M., Reinmuth, N., Shaheen, R. M., Bucana, C. D., and Ellis, L. M. The effects of angiopoietin-1 and -2 on tumor growth and angiogenesis in human colon cancer. Cancer Res., *61:* 1255–1259, 2001.
37. Kim, I., Kim, J. H., Moon, S. O., Kwak, H. J., Kim, N. G., and Koh, G. Y. Angiopoietin-2 at high concentration can enhance endothelial cell survival through the phosphatidylinositol 3′-kinase/Akt signal transduction pathway. Oncogene, *19:* 4549–4552, 2000.
38. Ahmad, S. A., Liu, W., Jung, Y. D., Fan, F., Reinmuth, N., Bucana, C. D., and Ellis, L. M. Differential expression of angiopoietin-1 and angiopoietin-2 in colon carcinoma. A possible mechanism for the initiation of angiogenesis. Cancer (Phila.), *92:* 1138–1143, 2001.
39. Zagzag, D., Hooper, A., Friedlander, D. R., Chan, W., Holash, J., Wiegand, S. J., Yancopoulos, G. D., and Grumet, M. *In situ* expression of angiopoietins in astrocytomas identifies angiopoietin-2 as an early marker of tumor angiogenesis. Exp. Neurol., *159:* 391–400, 1999.
40. Brown, L. F., Dezube, B. J., Tognazzi, K., Dvorak, H. F., and Yancopoulos, G. D. Expression of Tie1, Tie2, and angiopoietins 1, 2, and 4 in Kaposi's sarcoma and cutaneous angiosarcoma. Am. J. Pathol., *156:* 2179–2183, 2000.
41. Folkman, J., and D'Amore, P. A. Blood vessel formation: what is its molecular basis? Cell, *87:* 1153–1155, 1996.
42. Maxwell, P. H., Pugh, C. W., and Ratcliffe, P. J. Activation of the HIF pathway in cancer. Curr. Opin. Genet. Dev., *11:* 293–299, 2001.
43. Shen, B-Q., Lee, D. Y., Gerber, H-P., Keyt, B. A., Ferrara, N., and Zioncheck, T. F. Homologous up-regulation of KDR/Flk-1 receptor expression by vascular endothelial growth factor *in vitro*. J. Biol. Chem., *273:* 29979–29985, 1998.
44. Oh, H., Takagi, H., Otani, A., Koyama, S., Kemmochi, S., Uemura, A., and Honda, Y. Selective induction of neuropilin-1 by vascular endothelial growth factor (VEGF): A mechanism contributing to VEGF-induced angiogenesis. Proc. Natl. Acad. Sci. USA, *99:* 383–388, 2002.
45. Grunstein, J., Masbad, J. J., Hickey, R., Giordano, F., and Johnson, R. S. Isoforms of vascular endothelial growth factor act in a coordinate fashion to recruit and expand tumor vasculature. Mol. Cell. Biol., *20:* 7282–7291, 2000.
46. Yu, J. L., Rak, J. W., Klement, G., and Kerbel, R. S. Vascular endothelial growth factor isoform expression as a determinant of blood vessel patterning in human melanoma xenografts. Cancer Res., *62:* 1838–1846, 2002.